

41

INDUCED VORTICITY IN A HIGH DENSITY PLASMA

G. Lisitano

IPP III/4

Februar 1971

MAX-PLANCK-INSTITUT FÜR PLASMAPHYSIK
GARCHING BEI MÜNCHEN

MAX-PLANCK-INSTITUT FÜR PLASMAPHYSIK

GARCHING BEI MÜNCHEN

INDUCED VORTICITY IN A HIGH DENSITY PLASMA

G. Lisitano

IPP III/4

Februar 1971

Die nachstehende Arbeit wurde im Rahmen des Vertrages zwischen dem Max-Planck-Institut für Plasmaphysik und der Europäischen Atomgemeinschaft über die Zusammenarbeit auf dem Gebiete der Plasmaphysik durchgeführt.

INDUCED VORTICITY IN HIGH DENSITY PLASMA

G. Lisitano⁺

Association EURATOM - Max Planck Institut fuer
Plasmaphysik, 8046 Garching, Germany

Abstract: Plasma vortex tubes surrounding the core of a high density plasma are induced by means of a new model of rotating plasma beams. Hydromagnetic interpretation of the induced plasma vorticity is derived from the measured plasma streamlines.

The study of vorticity in magneto-fluid dynamics is of great interest in exploring the properties of both laboratory and stellar plasmas. As an example, the formal analogy between the behavior of vorticity in hydrodynamics and the behavior of magnetic fields in plasmas of infinite conductivity led to the concept of frozen magnetic lines of force in stellar plasmas.

But, besides the diffusion of magnetic field lines in plasmas of finite conductivity, the question of fluid vorticity in laboratory plasmas has not yet been sufficiently explored theoretically, while almost no experimental investigations have thus far been reported.

The new model of rotating plasma beams presented in this letter induces plasma vortex tubes around the core of a high density plasma. The reported data on plasma streamlines suggest a description of the plasma vorticity by means of a set of equations similar to

those describing the classical HELMHOLTZ theorems of hydrodynamics. On the other hand, this experiment discloses a new possibility of confining high density plasma by means of controlled induction of vortex tubes which surround the core of the plasma axisymmetrically.

As shown in Fig. 1a, this model is realized by means of six electrodeless L-sources of plasma /1/, each 2.6 cm i.d. and 8 cm in length, which are embedded in the walls of a 4.5 cm thick, 8 cm long ceramic cylinder whose interior diameter of 8 cm is not screened with metal.

The system, which is assembled inside a discharge tube, 17 cm i.d., is positioned in the linear section of a linear magnetic mirror (mirror ratio 1.2 : 1).

Each of the sources is excited with r.f. power up to 100 W, 2.4 Gc/s in C.W. operation.

As shown in Fig. 2, the accumulation of plasma occurs not along the axis of each plasma producing source, but in a new equilibrium position centered on the axis of the main discharge tube.

Electron densities $N_e > 10^{13} \text{ cm}^{-3}$, corresponding to cut-off of an ordinary 8 mm wave, have been obtained at the maximum available r.f. power level of 100 W fed to each of the six coils. The distribution of the electron energy was very Maxwellian, $T_e \approx 15 \text{ eV}$, with a flat temperature profile across the plasma column.

These measurements were made with the uniform magnetic field strength (extending 200 cm in the central part of the mirror) set at the maximum available value of 11 kG. Owing to the cut-off dimension of the six sources,

no r.f. power is radiated axially into the main vacuum tube; therefore almost complete burnout of the neutral gas is assured by the high concentration of r.f. power and by a capillary gas feed in the sources.

The working gas pressure at which the plasma can be maintained may be as low as $2 \cdot 10^{-5}$ torr. De-excitation of the sources raises the neutral gas pressure to $3 \cdot 10^{-4}$ torr, indicating neutral burnout of more than one order of magnitude. The discharge, besides being maintained for any value of magnetostatic field strength satisfying the condition $\omega_{ce} > \omega_{rf}$, has a remarkably low level of density fluctuations ($\langle n_e \rangle$) $< 5\%$. Spectroscopic measurements of the radiated light have shown a complete absence of impurity in the discharge.

Undoubtedly, in order to understand the intricate properties of this plasma source, a visualization of the plasma stream or potential lines would be of great help. Unfortunately, no method has thus far been available for measuring stream or potential lines in hydromagnetics.

However, as will be shown in the following, a map of the floating equipotential lines such as that shown in Fig. 1b corresponds qualitatively to a cross section of the plasma streamlines in steady state flow.

The floating potential lines of Fig. 1b were measured at a plasma cross section 80 cm distant from the source. Local variations of the floating potential in a Maxwellian plasma may be due to several factors, the most important of which are : i) loss of ions to the walls, ii) inertial

forces on rotating plasmas and iii) pressure gradient

∇p forces / 2 / .

The balancing or driving energy for such losses or forces is provided in this model by the rotating plasma beams. Under conditions of axial symmetry and of flat temperature profile of the plasma, configurations such as that of Fig. 1b are routinely mapped by means of the floating potential profiles I and II of Fig. 2, which are measured respectively along the radii I and II of Fig. 1b. From Fig. 1b one is tempted to write the following set of hydromagnetic equations:

$$1) \int_F \nabla \times V_I \, dF = \text{Const.} = K \int_F J_{II} \, dF$$

$$2) \quad \nabla \times V_I = K J_{II} \quad ; \quad \nabla V_I = 0$$

$$3) \quad V_I = E_I^* \times B_{II}$$

$$4) \quad \nabla E_I^* = - \frac{q}{\epsilon} = \Delta \psi$$

where V_I is the macroscopic plasma velocity transversal to the axial uniform magnetostatic field B_{II} ; J_{II} is the current density distribution due to the axial steady state flow of the excess charge of the quasi-neutral plasma; K is a dimensional constant; E_I^* is the transversal electric field due to the mentioned local variations of the plasma potential and takes account of all the usual terms of the equation of motion of hydromagnetics; q is the excess charge density of the quasi-neutral plasma, which may be derived from the Poisson equation $q / \epsilon = -\Delta \psi$, where ψ is the potential distribution associated with the parallel flow of the electrical excess charge.

Equation 1) is similar to the THOMSON theorem of hydrodynamics. As is well known, the three classical HELMHOLTZ theorems of vorticity in hydrodynamics can be derived from the Thomson theorem.

As a consequence of eq. 1), the formal analogy between the Helmholtz theorem of vorticity $\nabla \times V = \omega$;

$$\nabla V = 0 \quad (\text{where } \omega \text{ is the vorticity distribution})$$

and the equation of electromagnetics $\nabla \times B = J$;

$$\nabla B = 0 \text{ is extended by means of eq. 2) to hydromagnetics.}$$

One can therefore deduce the following statement:

" as in hydrodynamics a distribution of vorticity produces a velocity distribution and as in electromagnetics a distribution of current produces a distribution of magnetic field, in hydromagnetics a distribution of electric current produces a distribution of velocity".

In reality, both equations of hydrodynamic vorticity and of electromagnetics are valid for hydromagnetics.

However, assuming a fluid of low magnetic Reynolds number, the magnetic field induced from a current distribution

$\nabla \times B = J$ can be neglected in comparison to the applied magnetostatic field. At the same time, owing to the low value of viscosity in plasmas as compared to that of fluids or of dense neutral gas, the velocity distribution induced from the vorticity of a neutral plasma can be neglected relative to the velocity distribution due to $E_1^* \times B_{II}$ forces as stated by equation 3).

Thus the current J_{II} of eq. 1), which is interpreted as the current due to a stream of excess charges along the

applied magnetic field, corresponds to the sinks and to the sources of hydrodynamic vorticity.

In Fig. 1b sinks are indicated by a clockwise rotation of the streamlines corresponding to an axial flow of negative charges, while sources which are indicated by a counterclockwise rotation of the streamlines correspond to an axial flow of positive charges / 3 /.

Equation 2) follow immediately from eq. 1), but $\nabla V = 0$ can also be derived from the equation of mass conservation $\delta \rho / \delta t + \nabla \rho V = 0$ by assuming an isotropic and incompressible fluid $D\rho / Dt = 0$.

In order to relate the set of equations 1) - 4) to the flow configuration of Fig. 1b, one has to consider the boundary conditions of the discharge.

In hydromagnetics the boundary problem is complicated because of combined hydrodynamic and magnetoelectric effects.

However, the flow configuration of the plasma is controlled in this model by means of strong r.f. fields at the boundary of the plasma. These "controlled" boundary field effects are much larger than the previously mentioned "passive" boundary effects.

In particular, leakage r.f. fields through the interior of the large diameter of the plasma source, have a "wavy" field strength, as shown in Fig. 1b.

This undulating field has a strong stabilizing effect. This can be seen in Fig. 1b, where the induced vortices near the core of the plasma are disposed like KARMAN'S

vortex trail of hydrodynamics / 4 /.

According to KÁRMÁN's analysis a stable vortex pattern must have a geometry such that $h/l = 0.28$, where h and l are the distances between two vortices respectively across and along the flow direction. In Fig. 1b, although the geometry is circular rather than straight, the value of h/l is very close to that corresponding to the conditions of stable flow in hydrodynamics.

The analogy between hydrodynamic and hydromagnetic vorticity may be extended to the more important field of laminar isolation of solenoidal flow.

As a vorticity trail represents an increased resistance of hydrodynamic flow, an electric current trail such as that shown in Fig. 1b may represent a reduction of the transverse conductivity of the plasma.

This high confining effect of the induced hydromagnetic vorticity surrounding the core of the plasma is demonstrated by the steep radial profile of the plasma density shown in Fig. 1b and in Fig. 2 .

Measurements made with different gases have shown a gas number dependence of the radial position of the sinks and sources of Fig. 1b.

This is explained in the following by assuming that the azimuthal steady state flow perturbation (due to the azimuthal position of the rotating plasma beams) propagates transversally with the ALFVEN velocity: /

$$V_A = (B / \sqrt{\rho\mu}) \cos \theta$$

The azimuthal position of the six rotating plasma beams fixes the wavelength of the steady state flow perturbation.

Knowing the azimuthal velocity given by eq. 3), where E_{\perp}^* is given by $\nabla\psi$ (in Fig. 1b and Fig. 2, $\nabla\psi$ is of the order of 10^2 V/cm), one can deduce the frequency of the perturbation, f .

Assuming the radial distance between the sinks and sources as a standing wavelength λ , one can compare the wave velocity $V = f\lambda$ with V_A . Knowing the plasma density, the derived value of $B \cos \theta$, which represents the radial component of B , proves to be very close to the measured value of the axial non-uniformity of the applied magnetostatic field.

Acknowledgment : The autor wishes to thank M. Bergbauer, A. Capitanio, H. Häglsperger, A. van Heumen, A. Reiter and E. Rossetti for their highly professional engineer work.

References

- + Associate Professor of Magneto-Fluid Dynamics of the " Politecnico di Milano " , Italy .
- / 1 / G. Lisitano, M. Fontanesi and E. Sindoni
Appl. Phys. Lett. 16, 122 (1970)
- / 2 / For a Maxwellian plasma having a flat radial profile of temperature, the difference between floating and space potential can be considered as almost constant. The floating potential which is obtained for the condition $n_e V_e = n_i V_i$, is very sensitive to any local departure of charge neutrality of the quasi-neutral plasma and to any local variation of velocity distributions of the two plasma components. Extensive measurements on this subject will be reported elsewhere.
- / 3 / The distribution of excess charge streams axially with thermal velocity. For a directed current, due, for examples to an induced or to an electrode voltage, the solenoidal velocity distribution described by eq. 2) would break up in turbulence if the poloidal field associated with the current, became significant relative to the applied magnetostatic field.
- / 4 / Extensive measurements, to be reported elsewhere, have demonstrated that the floating potential configuration of Fig. 1b does not depend on the multi-mode distribution of the leakage r.f. field out of the plasma sources.

Figure Captions

- Fig. 1 a) System of six rotating plasma sources assembled symmetrically around the axis and close to the inside wall of a main discharge tube.
- b) Cross section of the plasma streamlines 80 cm distant from the sources.
- Fig. 2 Radial profiles of floating potential V_f , and of electron density N_e .

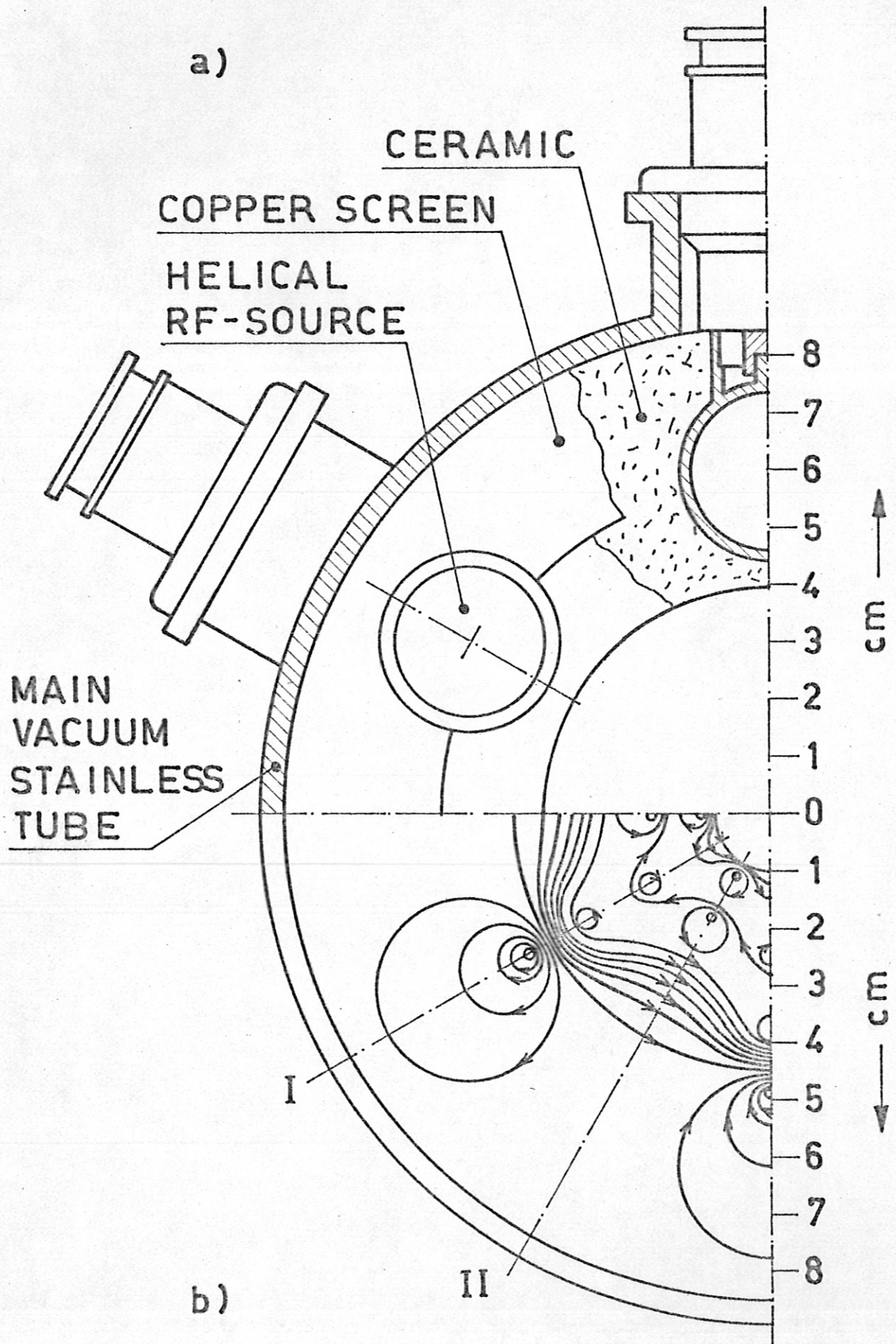


Fig.1

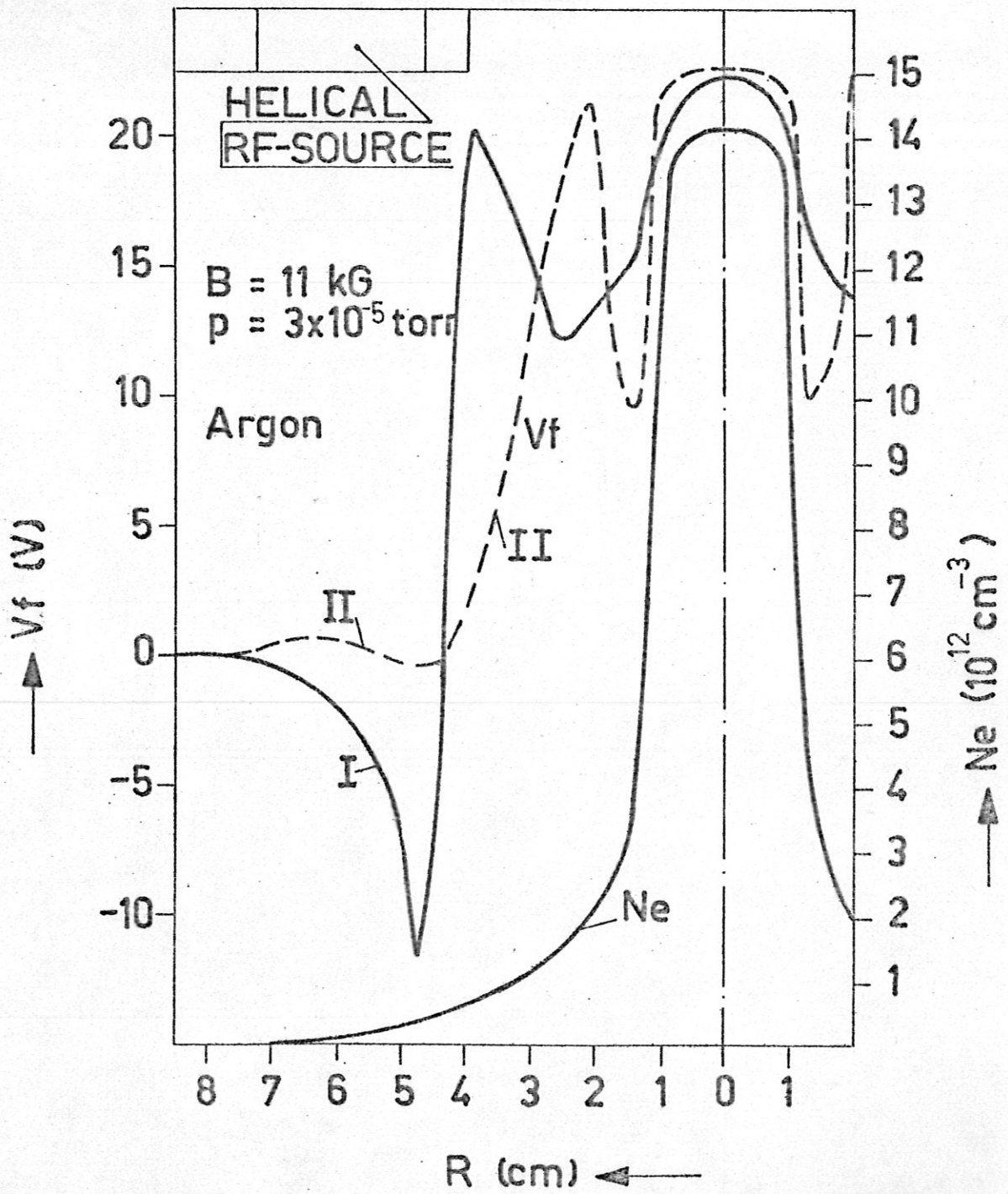


Fig.2